Polymer 50 (2009) 3478–3487

Contents lists available at ScienceDirect

Polymer

journal homepage: www.elsevier.com/locate/polymer

Ethylene vinyl acetate/layered silicate nanocomposites prepared by a surfactant-free method: Enhanced flame retardant and mechanical properties

Yaru Shi [a,1], Takashi Kashiwagi [b], Richard N. Walters [c], Jeffrey W. Gilman [b], Richard E. Lyon [c], Dotsevi Y. Sogah [a,*]

[a] Department of Chemistry and Chemical Biology, Cornell University, Ithaca, NY 14853, USA
[b] Materials and Products Group, Fire Research Division, National Institute of Standards and Technology, 100 Bureau Drive, Gaithersburg, MD 20899-866, USA
[c] Airport and Aircraft Safety Research and Development Division, William J. Hughes Technical Center, Federal Aviation Administration, Atlantic City International Airport, NJ 08405, USA

ARTICLE INFO

Article history:
Received 25 March 2009
Received in revised form
29 May 2009
Accepted 6 June 2009
Available online 12 June 2009

Keywords:
Nanocomposites
EVA
Flame retardancy

ABSTRACT

Exfoliated EVA/layered silicate nanocomposites were prepared by a masterbatch process using polymer-modified layered silicate instead of small molecule surfactant-modified clays. The nanocomposites exhibited improved mechanical properties and flame retardancy. Microscale flammability test showed that the heat release capacity (HRC) and total heat release (THR) were reduced by 21–24% and 16%, respectively. Radiant gasification studies revealed that the exfoliated EVA nanocomposites exhibited better improvements in flame retardant properties of EVA than did the corresponding intercalated nanocomposites. The peak mass loss rate of the exfoliated EVA nanocomposite containing about 5 wt% clay was reduced by 80% and the mass loss rate plot was spread over a much longer period of time. The mechanical and flammability tests revealed that the observed improvements in all the desirable properties were due to the presence of both the incorporated polymeric surfactant and the nanoclay.

1. Introduction

Ethylene vinyl acetate copolymers (EVA) are one of the important engineering polymers with broad applications, such as hot melt adhesives, packaging, wire and cable insulation and carpeting. These polymers are inflammable and for most of their applications, flame retardancy is an important attribute that needs to be achieved through the addition of flame retardants. Traditionally, aluminum trihydrate and magnesium hydroxide have been added as flame retardant additives at filling levels of 20–60 wt% [1]. The disadvantages of such high filling levels include poor processability, lack of product flexibility, and reduced toughness and clarity. Other flame retardant additives such as halogenated compounds are not preferred due to environmental concerns.

As a new class of flame retardant materials, polymer/silicate nanocomposites might avoid some of the problems noted above [2–11]. Morgan and Wilkie recently published a comprehensive book on flame retardant polymer nanocomposites, covering both fundamental theories and real examples [12]. For nanocomposites with homogeneous dispersion of inorganic nanofillers, improvement in flame retardancy and mechanical properties are realized at less than 5 wt% inorganic loading, with minimal adverse effect on processability. Among all the different inorganic nanofillers layered silicates draw the most attention, because of their obvious cost advantage and great potential in maintaining (or even improving) overall polymer properties.

Various groups have studied EVA/layered silicate nanocomposites [13–41]. They observed some improvement in flame retardancy and in some aspects of mechanical properties in cases where the clay platelets were reasonably dispersed [42]. Most of the EVA/clay nanocomposites reported so far were prepared either by mixing organically modified clay with EVA in solution or by melt extrusion. The surface modifiers are usually small organic molecule surfactants, such as alkylammonium and alkylphosphonium salts [12,15,16,19–22]. There are two major problems associated with the use of small molecule surfactants. First, these small molecules may not be able to give large enough clay intergallery expansion, which leads to intercalated or partially exfoliated morphology, and consequently less property improvement. Moreover, under certain processing conditions, such as melt extrusion, the decomposition of these volatile small molecules by Hofmann elimination reaction [43,44] results in the re-collapse of the clay stacks and poor exfoliation [16,18,21,45,46]. Second, small molecule surfactants may cause

* Corresponding author. Tel.: +1 607 255 4205; fax: +1 607 255 4137.
E-mail address: dys2@cornell.edu (D.Y. Sogah).
[1] Current address: Evonik Stockhausen Inc., 2401 Doyle Street, Greensboro, NC 27406, USA.

0032-3861/$ – see front matter © 2009 Elsevier Ltd. All rights reserved.
doi:10.1016/j.polymer.2009.06.013

Table 1
Compositions of EVA/MMT nanocomposites and their thermal properties.

Sample	Morphology[a]	Composition		T_g (obsd)[c] (°C)	T_m[d] (°C)	T_c[e] (°C)	ΔH_c[f] (J/g)
		Polymeric modifier (wt%)	MMT (wt%[b])				
EVA39	N.A.[h]	0	0	−31	50	33	9.96
EVA-1	Intercalated	PVAc (4)	0.9	−32	48	33	7.97
EVA-2	Intercalated	PVAc (8)	1.9	−34	48	33	8.21
EVA-5	Intercalated	PVAc (20)	5.9	−31	50	33	7.18
EVA-0	N.A.[h]	PVAc (20)	0	−32 (−21)[g]	48	32	7.70
EVA-NC1	Exfoliated	PVAc-1 (4)	0.84	−32	49	33	8.10
EVA-NC2	Exfoliated	PVAc-1 (8)	2.1	−33	49	32	8.50
EVA-NC5	Exfoliated	PVAc-1 (20)	5.6	−31	50	32	6.89
EVA-NC0	N.A.[h]	PVAc-1 (20)	0	−32 (−21)[g]	49	33	7.79

[a] Determined from XRD and TEM.
[b] Measured by TGA under nitrogen.
[c] Glass transition temperature from DSC (cooling cycle).
[d] Melting temperature from DSC (heating cycle).
[e] Crystallization temperature from DSC (cooling cycle). The T_m and T_c of EVA39 supplied by the vendor are: T_m 47 °C and T_c 28 °C.
[f] Heat of crystallization calculated from DSC plots (cooling cycle). The uncertainty in ΔH_c is ±5%.
[g] The calculated T_g using Fox equation (Fox TG. Bull. Am. Phys. Soc. 1956:1:123) was −21 °C.
[h] Not applicable.

early ignition in flame retardancy tests as previously reported [12,47].

In our previous work [48,49], we successfully prepared exfoliated EVA/silicate nanocomposites using a masterbatch process. A cationic vinyl acetate copolymer rather than a small molecule was used as the surface modifier to make the masterbatch, which was then mixed with EVA to yield well exfoliated nanocomposites. Detailed thermogravimetric analysis (TGA) revealed that the thermal stability of the nanocomposites prepared from the polymer-modified clay increased over those prepared using small molecule surfactants. The lower thermal stability of the nanocomposites prepared from clays modified with the typical alkylammonium surfactants was attributed to Hofmann elimination reaction that produced low molecular weight byproducts that were absent in the current nanocomposites [43,44,46,48]. Preliminary dynamic mechanical analysis (DMA) studies confirmed that incorporation of the polymeric modifier not only facilitated dispersion of the silicate layers but also influenced the storage moduli of the nanocomposites. Using the polymeric modifier also avoided the volatility problem during thermal processing and the early ignition problems in combustion associated with small molecule surfactants [12,47]. In this work, we report mechanical properties and flame retardancy measurements of the exfoliated EVA/montmorillonite (MMT) nanocomposites. The results reveal that the use of a polymeric surfactant provides enhancement of both mechanical properties and flame retardancy.

2. Experimental section

2.1. Materials and methods

Sodium MMT (hereafter referred to as simply MMT) with a cationic exchange capacity of 90 meq/100 g was supplied by Southern Clay Products. X-ray diffraction gave the *d* spacing of the interlayer as 1.2 nm. The EVA copolymer (Exxon Mobil's Escorene, UL05540EH2) used contained 39 wt% vinyl acetate (VA). The EVA nanocomposites used in our studies are listed in Table 1. The exfoliated EVA/MMT nanocomposites (EVA-NC1, EVA-NC2 and EVA-NC5) used for mechanical properties measurements and pyrolysis–combustion flow calorimeter (PCFC) studies were synthesized on a 20 g scale by blending EVA with a masterbatch nanocomposite, which was prepared by modifying MMT with a cationic vinyl acetate (VAc) copolymer using previously published procedures [48]. The cationic VAc copolymer (PVAc-1, Scheme 1) contained 1 mol% of (2-acryloxyethyl)trimethylammonium chloride (AETMC). MMT used in the preparation of this masterbatch was not modified with any other organic surfactant. The intercalated EVA/MMT nanocomposites (EVA-1, EVA-2 and EVA-5) used for comparison studies were synthesized similarly by blending EVA with a masterbatch nanocomposite, which was prepared by mixing PVAc homopolymer with MMT [48]. EVA-NC0, the control sample for EVA-NC5, was made by blending EVA with 20%(w/w) of PVAc-1. EVA-0, the control sample for EVA-5, was made by blending EVA with 20%(w/w) of PVAc homopolymer. All the control samples contained no clay. The samples for radiant gasification tests were prepared utilizing the same procedures but on a larger scale (200 g) [48]. The cationic comonomer contents of the masterbatches used in the gasification samples were as follows: PVAc-1, 1 mol% of AETMC and PVAc-2, 2 mol% of AETMC.

2.2. Characterization

2.2.1. X-ray diffraction

X-ray diffraction (XRD) was performed on powder samples on a Scintag X-ray Diffractometer in theta–theta geometry using Cu Kα radiation ($\lambda = 1.54$ nm) operated at 45 kV and 40 mA. The scanning speed and the step size were 3°/min and 0.02° two theta, respectively.

2.2.2. Thermal analysis

Thermogravimetric analysis (TGA) was measured under N_2 flow on a TA thermogravimetric differential thermal analyzer at a heating rate of 10 °C/min. Differential scanning calorimetry (DSC) was carried out under N_2 flow on a TA instrument. Each sample was first equilibrated at 200 °C and then cooled down to −70 °C at 10 °C/min ramp. The cooled sample was held at −70 °C for 10 min before it was heated to 130 °C at 10 °C/min ramp. The sample was maintained at that temperature for 10 min and then cooled down to −70 °C at a scan rate of 10 °C/min. The second heating and cooling cycles were recorded.

2.2.3. Mechanical properties' measurements

Mechanical properties were measured using an Instron instrument at 21 °C and 65% humidity. The crosshead speed was 50 mm/min. The dumbbell-shaped specimens were prepared by injection molding at 81 °C and under air pressure of 80 psi. The mold temperature was set at 41 °C. The dimensions of the center part of the dumbbell were 25 mm by 5 mm by 1.4 mm. The data reported

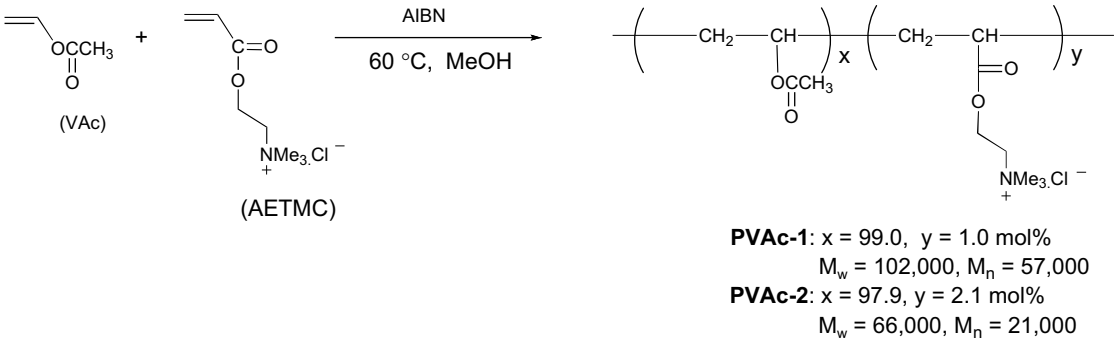

Scheme 1. Synthesis of the cationic PVAc copolymers.

were an average of 5 runs. The typical uncertainties (2 sigma) were: Strength at Yield: ±10%; Elongation at Yield: ±5%; Young's modulus: ±15%; Toughness: ±10%.

2.2.4. Microscale combustion calorimetry

Small scale flammability tests were carried out on pyrolysis–combustion flow calorimeter (PCFC, Govmark, Farmingdale, New York, Model MCC-1). The samples were tested according to ASTM D7309-07. Approximately 5 mg of each sample was weighed on a microbalance and placed in a sample cup. The sample cup was placed on a platform with an embedded thermocouple and raised into the PCFC heated tube that was purged with nitrogen. The sample was heated at 1 °C/s to a maximum temperature of 900 °C. The gaseous decomposition products mix in the gas stream with oxygen prior to entering the combustion section of the PCFC where they are completely oxidized. The water was scrubbed from the gas stream, and the oxygen concentration and flow rates were measured. Heat release rate (HRR) in Watts per gram of sample (W/g) was calculated from the oxygen depletion measurements. Heat release capacity (HRC) in J/g K was obtained by dividing the sum of the peak HRR by the heating rate in K/s. The total heat release (THR) in kJ/g was obtained by integrating the HRR curve. The char yield was obtained by weighing the sample before and after the test. Values reported herein were the average of 3 tests. The experimental error was ±5% (2 sigma).

2.2.5. Gasification studies[2]

The EVA and EVA nanocomposites samples were compression molded at 81 °C and 3000 psi for 10 min to obtain round disk specimens whose dimensions were 7.50 cm (diameter) by 8.23 mm (thickness). Radiant gasification experiments were performed on the radiative gasification apparatus (RGA) at NIST. The instrument is similar to a cone calorimeter but permits the study of gasification of samples in a nitrogen atmosphere by measuring mass loss rate and back-side temperature of the samples, and allows video to be taken of the pyrolysis of the samples exposed to a fire-like heat flux. No burning is involved. It is suited for evaluating small flame retardancy differences and mechanistic studies of condensed phase flame retardant effects because it decouples the condensed phase deposition process from the gas phase combustion and radiative heat feedback from the flame [50,51]. A detailed discussion of the NIST instrument can be found in a previously published paper [50]. In this study, mass loss rate data and video were collected at a heat flux of 50 kW/m^2. The standard uncertainty of the measured mass loss was ±10% (2 sigma).

[2] Part of this work was carried out by the National Institute of Standards and Technology (NIST), an agency of the US government and by statute is not subject to copyright in USA. The identification of any commercial product or trade name does not imply endorsement or recommendation by NIST. The policy of NIST is to use metric units of measurement in all its publications, and to provide statements of uncertainty for all original measurements. In this document, however, data from organizations outside NIST are shown, which may include measurements in non-metric units or measurements without uncertainty statements.

3. Results and discussion

3.1. Compositions of the EVA/MMT nanocomposites and their thermal properties

The exfoliated EVA/MMT nanocomposites (EVA-NC1, EVA-NC2 and EVA-NC5) were prepared by solution blending of EVA with a masterbatch nanocomposite. The masterbatch nanocomposite in turn was prepared by modifying MMT with cationic PVAc copolymers designated PVAc-1 or PVAc-2 in our study. The synthesis route for the two cationic PVAc copolymers is shown in Scheme 1 and the actual procedure was published previously [48].

The masterbatch nanocomposite was completely exfoliated as a result of the strong electrostatic interactions of the pendant cationic ammonium groups in the copolymer with the anionic silicate surface. This prevented the clay layers from aggregating. Detailed XRD and TEM of these exfoliated nanocomposites were reported previously [48]. In order to determine the effect of exfoliation on the properties of the nanocomposites, we prepared analogous intercalated nanocomposites (EVA-1, EVA-2 and EVA-5) that contained approximately the same amount of clay by replacing the cationic copolymer with PVAc homopolymer.

Fig. 1 compares the XRD plots of MMT, EVA-NC5 and EVA-5. While EVA-NC5 appeared to be exfoliated as judged by the absence of any peak in the XRD pattern, EVA-5 gave a peak consistent with silicate layers with *d* spacing of 2.1 nm, which indicates an intercalated structure. The XRD results agreed well with the TEM of both EVA-NC5 and EVA-5 previously reported [48].

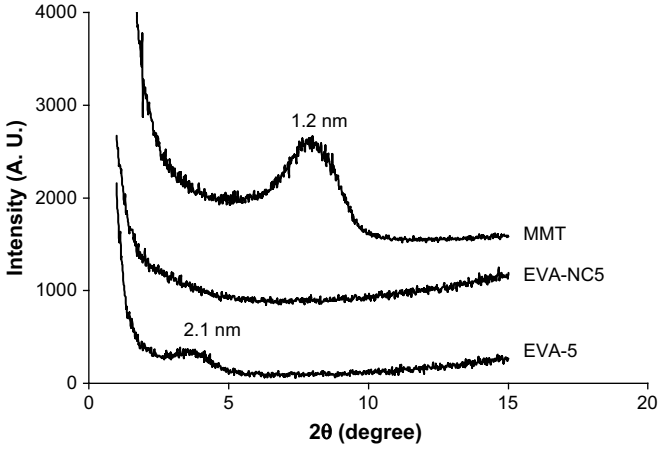

Fig. 1. XRD patterns of MMT, EVA-5 and EVA-NC5.

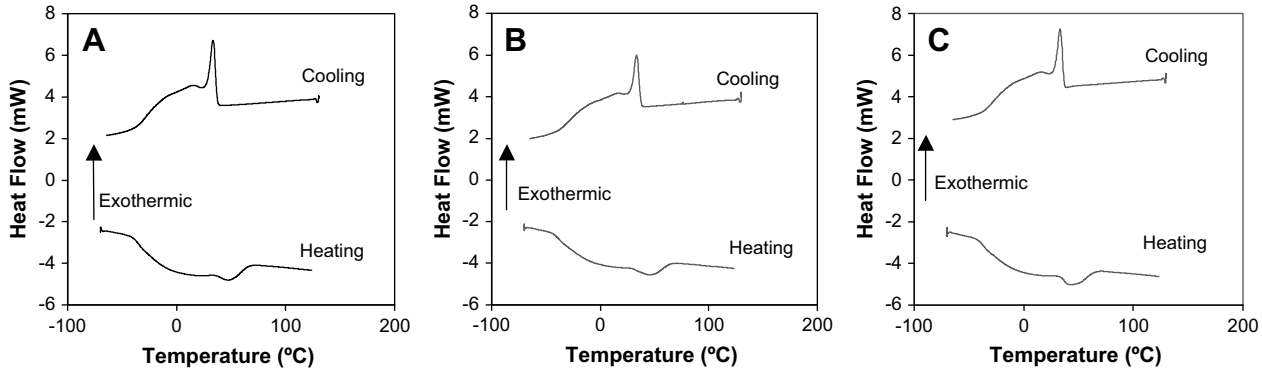

Fig. 2. DSC cooling and heating thermograms of EVA (A), EVA-5 (B) and EVA-NC5 (C).

In order to determine the contributions of the polymeric modifiers to the properties of the nanocomposites, samples containing no clay were prepared by separately blending EVA with PVAc to give EVA-0 and with PVAc-1 to give EVA-NC0 as the controls for EVA-5 and EVA-NC5, respectively. The compositions and the thermal properties of all the samples are summarized in Table 1.

Fig. 2 shows the DSC curves for EVA, EVA-5 and EVA-NC5. ΔH_c values obtained from the area under the crystallization peak are listed in Table 1. The DSC thermograms revealed both glass transition (T_g), melting (T_m) and crystallization (T_c) temperatures that appeared to be independent of composition for all the samples, as shown in Table 1. It is evident from the data that the presence of the polymeric modifiers (PVAc or PVAc-1), even in the absence of clay, resulted in decreased crystallinity of EVA. Thus, the ΔH_c values decreased from 9.96 J/g for EVA to 7.70 J/g for EVA-0 and 7.79 J/g for EVA-NC0. The addition of MMT resulted in further decrease in crystallinity as is evident from the fact that both EVA-5 and EVA-NC5 showed reduced ΔH_c values compared with the corresponding controls EVA-0 and EVA-NC0, respectively. All the nanocomposites gave ΔH_c values smaller than the value for EVA. The results suggest that the increase in mechanical properties discussed later is most likely due to nanoscale reinforcement by the clay and not to increased crystallinity resulting from nucleation by the clay.

3.2. Mechanical properties

Perusal of the mechanical properties data summarized in Table 2 revealed that, relative to neat EVA, all the EVA/MMT nanocomposites exhibited some improvement in both yield strength and Young's modulus. Even the control samples EVA-0 and EVA-NC0 showed higher yield strength and Young's modulus than EVA. Although the improvement was accompanied by a decrease in percent elongation at yield, it is apparent from the values obtained for the controls that this decrease was caused by the presence of the PVAc and PVAc-1 in the masterbatches.

Plots of tensile strength and Young's modulus vs. clay content (Figs. 3 and 4) showed that both properties increased with increasing clay content. The mechanical properties data summarized in Table 2 and Figs. 3–6 revealed that, in general, the exfoliated EVA/MMT nanocomposites exhibited higher improvements in mechanical properties at all clay contents. For example, the tensile strength and Young's modulus for the exfoliated EVA-NC5 were almost double and triple that for EVA, respectively (Table 2, columns 2 and 3).

It is not uncommon for polymer/clay nanocomposites to be strengthened and stiffened simultaneously as the above data in our system show. However, these improvements are usually accompanied by trade-offs, such as reduced toughness. Fig. 5 shows that elongation at yield decreased for all the nanocomposites with increasing clay content. However, the decrease was less for the exfoliated nanocomposites. Although elongation is a good measure of ductility of materials, toughness, which can be approximated by the area under the stress–strain curve, is generally considered to be a more accurate measure. Fig. 6 indicates that upon addition of 1% clay the toughness of EVA first decreased from 9.8 to 7.7 MPa. However, as the clay content increased, the toughness began to increase. In particular, the exfoliated nanocomposite at a clay

Table 2
Mechanical properties of EVA/MMT nanocomposites.[a]

Samples	Yield strength (MPa)	Modulus[b] (MPa)	Percent elongation[c]	Toughness[d] (MPa)
EVA	3.08	1.60	391	9.76
EVA-1	3.72	2.65	247	7.69
EVA-2	3.79	2.66	236	6.90
EVA-5	5.44 (+76%)[e] (+46%)[f]	4.07 (+155%)[e] (+42%)[f]	189 (−52%)[e] (−18%)[f]	7.13 (−27%)[e] (+5%)[f]
EVA-0	3.72 (+21%)[e]	2.88 (+80%)[e]	232 (−41%)[e]	6.79 (−30%)[e]
EVA-NC1	3.59	2.25	267	7.68
EVA-NC2	4.48	3.21	244	8.44
EVA-NC5	6.11 (+98%)[e] (+65%)[g]	4.67 (193%)[e] (+57%)[g]	212 (−46%)[e] (−9%)[g]	9.17 (−6%)[e] (+24%)[g]
EVA-NC0	3.71 (+21%)[e]	2.98 (+87%)[e]	232 (−41%)[e]	7.39 (−24%)[e]

[a] Mechanical properties measured by Instron at a crosshead speed of 5 mm/min. The typical uncertainties were: Strength at Yield: ±10%; Elongation at Yield: ±5%; Young's modulus: ±15%; Toughness: ±10%. The numbers in parentheses are the percent changes in the mechanical properties values.
[b] Young's modulus.
[c] Percent elongation at yield.
[d] Calculated from area under the stress–strain curve.
[e] Calculated with respect to the corresponding values for EVA.
[f] Calculated with respect to the corresponding values for EVA-0.
[g] Calculated with respect to the corresponding values for EVA-NC0.

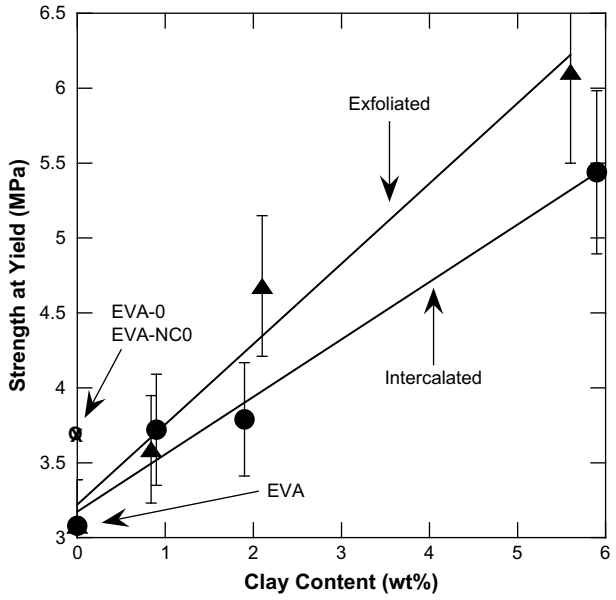

Fig. 3. Tensile strength vs. clay content.

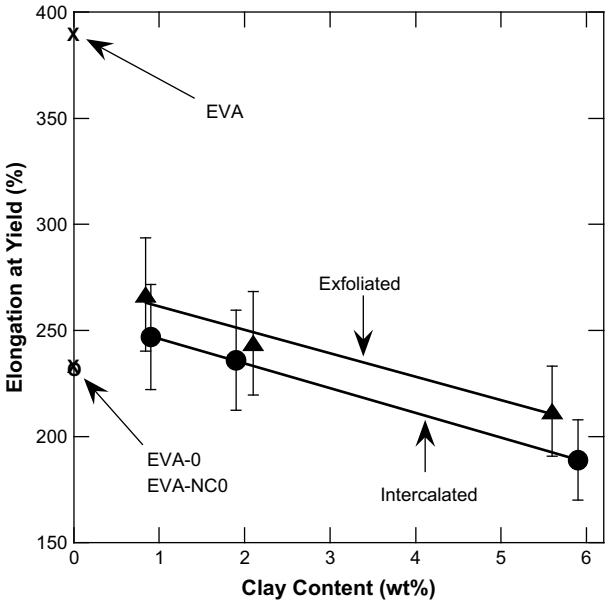

Fig. 5. Elongation at Yield vs. clay content.

content of approximately 5 wt% (EVA-NC5) gave a toughness value of 9.2 MPa, which is very close to the toughness value of neat EVA (9.8 MPa), within experimental uncertainty. The intercalated nanocomposite behaved similarly but the increase was much less than observed for the exfoliated nanocomposite. These results clearly suggest that, contrary to expectation, the presence of clay in a nanocomposite, especially, that prepared using a pre-exfoliated masterbatch can have a beneficial effect on toughness. Furthermore, the effect is more pronounced in the exfoliated EVA nanocomposites than in the corresponding intercalated ones at all the clay loadings investigated. The different behavior exhibited by the various nanocomposites can therefore be attributed to the higher interface areas due to the fine dispersion of the silicate layers in the polymer matrix; the higher the dispersion is, the better the improvement in properties become. These observations agree well with our earlier results obtained using DMA [48], which showed that while the storage moduli above T_g improved for both types of nanocomposites, the exfoliated nanocomposites generally exhibited higher storage moduli than the corresponding intercalated nanocomposites at the same clay loading.

Since the masterbatch process introduced a polymeric modifier together with the clay, it was necessary to independently determine the contribution of the incorporated PVAc and PVAc-1 to the changes in the mechanical properties. We, therefore, measured the tensile properties of the control samples that contained no clay. The results in Table 2 showed that the tensile properties of the two control samples EVA-0 and EVA-NC0 were similar, suggesting that minor differences in the structure and composition of the polymeric modifiers (PVAc vs. PVAc-1) did not significantly affect the

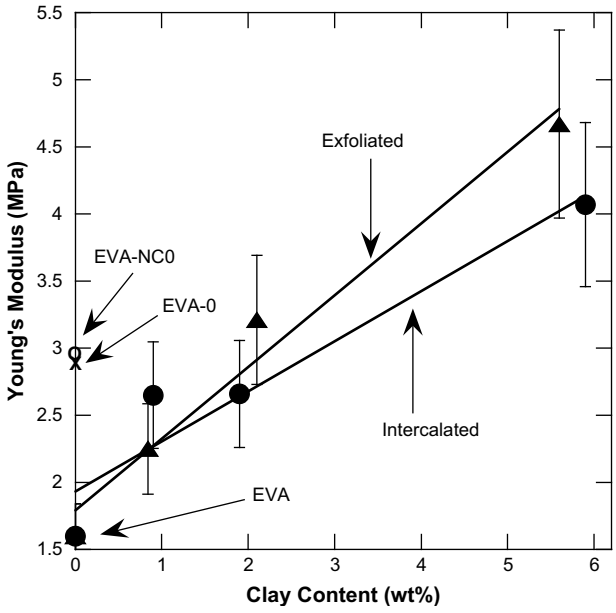

Fig. 4. Young's modulus vs. clay content.

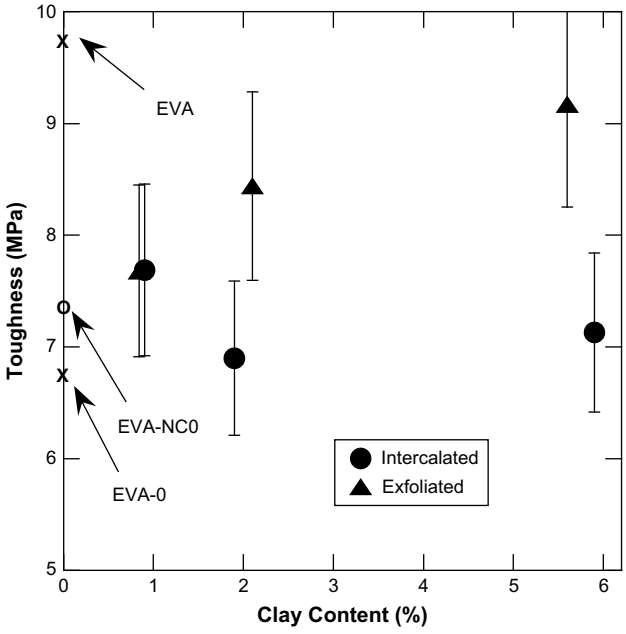

Fig. 6. Toughness vs. clay content.

mechanical performance. The tensile strength of the polymer blends (EVA-0 and EVA-NC0) increased by 21% while Young's modulus increased by more than 80% over the corresponding values for neat EVA. In contrast, toughness decreased by 30% for EVA-0 and 24% for EVA-NC0 but went back up upon addition of clay. Further examination of the data for the nanocomposites EVA-5 and EVA-NC5 revealed that the tensile strength, Young's modulus and toughness all increased relative to the values for the corresponding control samples. In every case, the improvement, as shown by the numbers in parentheses in Table 2, was even larger when compared to EVA. The results suggest that the observed improvements in the mechanical properties are due to the presence of both the polymeric modifiers and the nanoclay. In addition, exfoliation led to better improvements as evidenced by EVA-NC5 giving consistently higher values in every case than did the intercalated EVA-5.

Toughness, as a total effect parameter, reflects the influence of both strength and elongation. Since the tensile strength increased with increasing clay content, the reduced toughness had to be due to reduction in elongation. Comparing the toughness values of neat EVA with those of the corresponding nanocomposites, it is clear that the presence of only PVAc reduced the toughness value, but the incorporation of both PVAc and nanoclay led to increased toughness. Thus, for EVA-NC5, the toughness was 24% higher than that of the control sample, EVA-NC0. These results confirm that the decrease in elongation noted earlier is almost solely due to the presence of the PVAc and PVAc-1 modifiers.

As pointed out earlier, addition of PVAc, an amorphous polymer, to EVA resulted in reduction of the crystallinity of EVA. This might be expected to lead to higher elongation but lower strength and lower modulus. However, because PVAc is a higher T_g material, its incorporation into EVA might have the opposite effect, that is, lead to higher strength and modulus but lower elongation. This is borne out by the mechanical properties of EVA-0 and EVA-NC0 as both exhibited higher tensile strengths and moduli but lower percent elongation and, consequently, lower toughness than EVA. It appears that the presence of the clay rather compensated for any reduction in toughness caused by the polymeric modifier in the masterbatch, leading to an overall improvement in toughness, especially, for the exfoliated nanocomposite. We have, therefore, accomplished the rare but much-sought-after goal of imparting increased mechanical properties without the usual trade-offs, demonstrating a unique characteristic of preparing nanocomposites by the masterbatch approach.

3.3. Microscale combustion calorimetry

Cone calorimetry is a commonly used approach to study flame retardancy and quantitatively measure heat release rate (HRR). However, it requires large quantities (25–100 g) of materials for accurate and reproducible determinations. Lyon and Walters at FAA developed the pyrolysis–combustion flow calorimeter (PCFC), which measures flammability of materials on milligram quantities [52–56]. They showed that the heat release capacity (HRC) measured by PCFC was proportional to the flaming HRR measured by conventional cone calorimeters and, therefore, could be a reasonable estimate of fire hazard, albeit using small quantities of samples. For most commercial polymers, they found a good correlation between the HRR obtained using the PCFC and regular cone calorimeters. However, such a correlation has not been hitherto established for polymer/inorganic nanocomposites. The work described herein is, therefore, among the earliest attempts to apply PCFC to polymer/MMT nanocomposites [57,58]. The detailed design of the PCFC is described in Lyon and Walters' patents [52,53] and published papers [54–56].

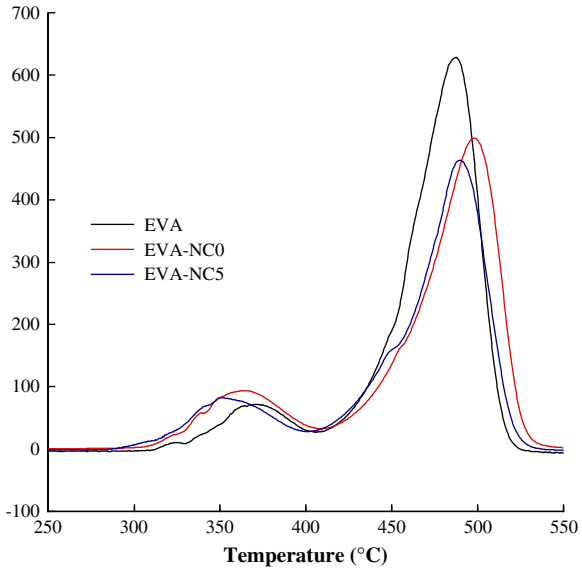

Fig. 7. HRR vs. temperature (°C) for EVA, EVA-NC5 and EVA-NC0.

Using the PCFC, we found that the HRR plots for EVA, EVA/MMT nanocomposites and EVA/PVAc blends were composed of two peaks as shown for EVA, EVA-NC5 and EVA-NC0 in Fig. 7. The first peak occurred between 351 and 369 °C, which corresponds to combustion of vinyl acetate units, or more specifically, to deacetylation of EVA. The second peak occurred between 485 and 499 °C and represented combustion of ethylene units and the polyene backbone. These are consistent with the thermal behavior of the materials reported earlier [48].

The HRC values, obtained as sum of the two peak HRR values, are summarized in Table 3. Neat EVA gave the highest HRC of 692 J/g K and the highest HRR peak of 628 W/g (peak 2, Fig. 7). The control sample EVA-0, which contained 20% PVAc, gave HRC value of 603 J/g K^{-1} while EVA-NC0 gave 581 J/g K. These values differ by only 3.6%, which is within the ±5% error limit. Addition of clay led to further reduction in HRC, with the nanocomposites that contained the highest amount of clay giving the lowest HRCs. The values for EVA-NC5 (544 J/g K) and EVA-5 (527 J/g K) differ by 3% (uncertainty, ±5%) but both are lower than those of the corresponding control samples. However, the reduction of HRC upon addition of clay appears to mainly reflect the reduction in the amount of polymer due to the presence of the clay, that is, a dilution effect.

THR, calculated from the total area under the HRR peaks, is another important parameter used to evaluate fire hazard. Both EVA-5 and EVA-NC5 gave THR values of 29.0 kJ/g and 29.3 kJ/g, respectively, corresponding to about 16% reduction in the THR of EVA. However, these values of THR are not significantly different

Table 3
PCFC results of EVA nanocomposites.

Samples	MMT[a] (wt%)	Max HRR temp (°C)		Char (%)	HRC[b] (J/g K)	THR (kJ/g)
		T_1	T_2			
EVA	0	369	488	0	692	34.5
EVA-5	5.9	355	490	6.1	527	29.0
EVA-0	0	365	499	0.4	603	31.9
EVA-NC5	5.6	351	490	5.6	544	29.3
EVA-NC0	0	364	498	0.6	581	31.4

[a] Measured by TGA under nitrogen.
[b] Obtained as sum of the two peak HRR values. The uncertainties in the HRC and HRR values ±5% (one standard deviation).

Table 4
Curve-fitting results of the multi-peak PCFC data.

Samples	MMT[a] (wt%)	Total acetate[b] (wt%)	Ethyne–ethylene[c] (wt%)	Deacetyl[d] peak 1 (%)	Ethyne–ethylene[e] peak 2 (%)	HR[f] (deacetyl) (kJ/g)	HR[f] (ethyne–ethylene) (kJ/g)	THR (kJ/g)
EVA	0	27	73	6	94	2.1	32.4	34.5
EVA-5	5.9	34	60	13	87	3.8	25.2	29.0
EVA-0	0	36	64	14	86	4.3	27.7	31.9
EVA-NC5	5.6	34	60	13	87	3.9	25.4	29.3
EVA-NC0	0	36	64	15	85	4.5	26.8	31.4

[a] Measured by TGA under nitrogen.
[b] Estimated as sum of the acetate groups in EVA and PVAc.
[c] Estimated from the ethylene in EVA and ethyne formed upon deacetylation of total VAc.
[d] From the area under peak 1 due to deacetylation event.
[e] From the area under peak 2 due to combustion of the polyene–polyethylene backbone.
[f] Heat release calculated from the relative areas under the two peaks and appropriate THR.

from the THR for EVA-0 and EVA-NC0 within the uncertainty of ±10% (2 sigma). As a comparison, Duquesne et al. reported higher THR value for EVA nanocomposites containing 5 wt% clay [25], while Zanetti et al. observed 11% reduction in THR for EVA nanocomposites of the same clay loading [17].

The PCFC results showed that the intercalated and the exfoliated EVA nanocomposites gave similar HRC and THR values, within experimental uncertainty. This suggests that PCFC is not able to conclusively distinguish between the flame retardancy characteristics of the exfoliated nanocomposites from those of the intercalated ones, contrary to previous results obtained using conventional cone calorimetry that suggested that extent of exfoliation affected the flame retardancy [1,47]. In our opinion, the apparent discrepancy is probably due to the small sizes of the specimens utilized in PCFC. The difference between the two types of nanocomposites observed in conventional cone calorimeter measurements was attributed to a "labyrinth" effect of the clay layers. The reassembly of the clay layers form a carbonaceous charred surface, which acts as a barrier to slow down the diffusion of volatile combustibles into the gas phase and the conduction of heat into the sample. This barrier effect of the clay particles would be very difficult to detect in measurements on the milligram quantities of samples required for the PCFC test.

The THR discussed above resulted from two events, deacetylation and combustion of the resulting polyene-ethylene backbone. Because of the overlap between the two peaks a curve-fitting program was utilized to deconvolute the peaks in order to assess the relative contribution of the two components. The results are presented in Table 4.

For neat EVA, the first peak from deacetylation accounted for 6% of the THR while polyethylene and the resulting polyene backbone (second peak) accounted for the remaining 94%. For the blend (EVA/PVAc = 80/20, EVA-0), the deacetylation contribution rose to 14% and, consequently, the contribution from ethylene–polyene dropped to 86%. For EVA-NC0 the VAc contribution was 15% and polyethylene–polyene contribution was 85%. The THR values of both blends were smaller than the value of neat EVA. Hence, the combustion of the polyethylene–polyene backbone accounted for 85–94% of the THR although the estimated weight fraction of ethyne–ethylene in the backbone was 0.60–0.73 (Table 4, columns 3 and 4). The results further revealed that the beneficial effect of clay on THR was due to the effect on both PVAc and polyethylene–polyene phases with a more significant effect being due to suppression of heat release from the polyethylene–polyene units. Despite the morphology difference, EVA-5 and EVA-NC5 behaved very similarly. This is consistent with their thermal properties discussed earlier and indicates that the reduced cone HRR of the nanocomposites discussed in the next section is simply due to a barrier effect.

In the flammability tests described above, the samples were first decomposed in a pyrolysis tube under N_2 purge before the combustible gases mixed with O_2 in the combustion furnace. This design avoided any complication from gas phase combustion, such as heat feedback, and obscuration of the sample surface from the flame. In this sense, the design is similar to the gasification device described by Gilman et al. [18] and Zanetti et al. [17]. In experiments performed in air using conventional cone calorimetry it is difficult to eliminate the influence of gas phase combustion.

In order to obtain flammability information in the presence of possible complications from gas phase combustion the PCFC measurements were performed in air on the nanocomposites containing the highest clay content (EVA-5 and EVA-NC5) and the corresponding controls (EVA-0 and EVA-NC0). The results, summarized in Table 5, show that the THR values measured in air were, in all cases (except for EVA), slightly higher than those obtained in nitrogen while pyrolysis residue (char yield) was slightly lower. This suggests that the organic component of the nanoclay, which is oxidatively stable under anaerobic conditions, is being oxidized (combusted) during the aerobic PCFC experiment. In addition, the combustion occurred at lower temperatures in air than in nitrogen for all the samples except EVA-NC5.

The first peak (deacetylation temperature) for each nanocomposite occurred at approximately the same temperature as that for the corresponding control sample. This suggests that the presence of oxygen during heating had little or no effect on deacetylation. However, the temperature at which polyene–polyethylene backbone combustion occurred (T_2) was higher for the nanocomposites than for the corresponding control samples. Thus, T_2 for EVA-NC5 was 16 °C higher than for EVA and 26 °C higher than for the control EVA-NC0. Similarly, T_2 for EVA-5 was 17 °C higher than for EVA-0 but only 1 °C higher than for EVA. This delayed polyethylene–polyene combustion peak might be related to oxygen diffusion shielding effect of the nanoclay layers in the nanocomposite. This observation agrees well with the delayed thermal oxidation temperature reported previously by others [1,16,22,42].

Table 5
PCFC results of selected EVA nanocomposites in air.

Samples	MMT[a] (wt%)	Char (wt%)	THR (kJ/g)	Max HRR temp (°C)	
				T_1	T_2
EVA	0	0	34.5	361	477
EVA-0	0	0	32.4	356	461
EVA-5	5.9	5.0	30.5	351	478
EVA-NC0	0	0	31.9	361	467
EVA-NC5	5.6	4.9	30.4	364	493

[a] Measured by TGA under nitrogen.

Table 6
Compositions of the EVA nanocomposites and control samples for gasification study.

Sample	Designation	Composition		Morphology
		Polymeric modifier (wt%)	MMT (wt%)	
EVA	A	0	0	
EVA/MMT	B	0	5	Microcomposite
EVA-0[a]	C	PVAc (20)	0	
EVA-5	D	PVAc (20)	5	Intercalated
EVA-NC5B[b]	E	PVAc-2 (20)	5	Mostly exfoliated
EVA-NC5[c]	F	PVAC-1 (20)	5	Fully exfoliated

[a] Control for EVA-5.
[b] Prepared from a masterbatch containing 24.9 wt% PVAc-2, a cationic PVAc containing 2 mol% of cationic moieties.
[c] Prepared from a masterbatch containing 21.5 wt% PVAc-1, a cationic PVAc containing 1 mol% of cationic moieties. The structures of PVAc-1 and PVAc-2 are shown in Scheme 1.

3.4. Gasification

The gasification tests were performed using the radiative gasification apparatus (RGA) developed at NIST. The RGA is similar to the cone calorimeter. However, unlike the cone calorimeter, the pyrolysis of samples occurs in a nitrogen atmosphere and, therefore, condensed phase pyrolysis and gas phase combustion are decoupled. Kashiwagi et al. used the RGA to obtain flame retardancy data for PA-6(nylon-6)/MMT nanocomposites [51]. They found that the reduction in HRR was mainly due to changes in the condensed phase rather than in the gas phase. The RGA allows measurement of mass loss rate during the pyrolysis experiment. Mass loss rate reflects the loss of fuel from the condensed phase into the gas phase and has been shown to be directly related to heat release rate measured in the cone calorimeter.

In this study six samples were tested (Table 6): EVA (A), EVA/MMT microcomposite (B), EVA-0 (C), EVA-5 (D), EVA-NC5B (E) and EVA-NC5 (F). The clay particles in the sample B (microcomposite) were neither intercalated nor exfoliated. EVA-NC5B was prepared from cationic PVAc (PVAc-2) that contained almost twice as much cationic moiety as in PVAc-1 used for EVA-NC5 discussed in the earlier sections of this paper. This nanocomposite (EVA-NC5B) was mostly exfoliated but contained some clay bundles as is evident from the TEM in Fig. 8. The less-than-complete exfoliated morphology was attributed to the increased polarity of the PVAc-2 copolymer due to the presence of the higher amount of the cationic comonomer, which rendered PVAc-2 somewhat immiscible with EVA. Indeed, we observed phase separation during preparation of the sample [48].

The mass loss rate plots are shown in Fig. 9. The video images of the char after gasification tests are shown in Fig. 10. In Fig. 9, neat EVA gave a typical mass loss rate curve of a pure polymer which was spread over 482 s. A thin layer of residue was left after the gasification (Fig. 10A). The plot showed a dip at about 335 s. The existence of the dip has also been reported by others and may be related to the polymer melting during the gasification test [51]. The peak mass loss rate was around 42 g/m^2 s. The mass loss rate curve of EVA-0 was almost identical to that of EVA. At the end of gasification experiment a thin grey layer of residue was left as shown in Fig. 10C. There were a few big bubbles and a lot of small bubbles left on the layer of residue. Addition of 5 wt% clay to EVA to form EVA/MMT microcomposite (sample B) led to a slight decrease in the peak mass loss rate and almost complete disappearance of the dip. The residue from this sample looked more like clay residue rather than polymer and there were numerous cracks on the thin layer of residue (Fig. 10B). Overall, the gasification curves of the control samples (EVA, EVA-0, EVA/MMT) were very similar.

The intercalated nanocomposite (EVA-5, sample D) behaved differently (Fig. 9, curve D). Not only did the dip disappear completely, the peak mass loss rate decreased by about 40% to 28 g/m^2 s and the mass loss rate curve was spread over a longer period (526 s). As shown in Fig. 10D, the grey residue covered the whole bottom of the container and showed numerous big cracks. This result indicates that although the intercalated silicate layers helped to form protective carbonaceous layers on the surface of the molten polymer the protection was not good enough to cover the surface completely and the EVA polymer was mostly burned.

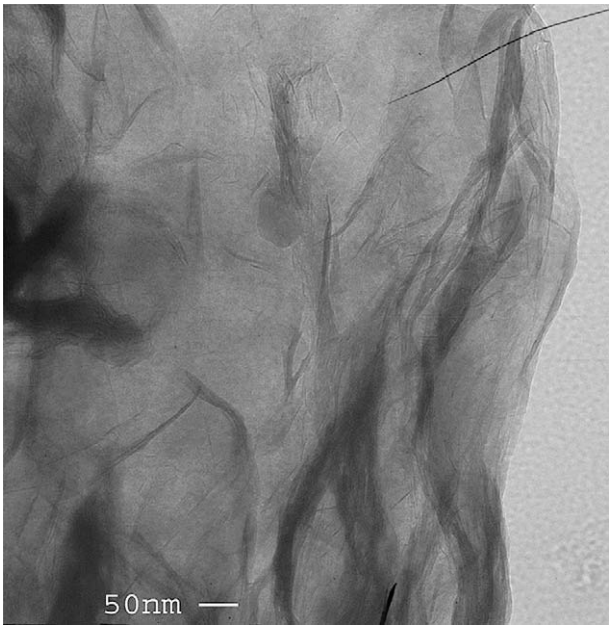

Fig. 8. TEM image of EVA-NC5B.

The completely exfoliated nanocomposite (EVA-NC5, sample F) gave the lowest peak mass loss rate (9 g/cm^2 s, 80% reduction (Fig. 9, curve F) compared to EVA Fig. 9, (curve A)) and the longest gasification period (1238 s). The video images (Fig. 10F) showed large amounts of black char-like residues in the pan. In comparison, the peak mass loss rate for the mostly, but not completely, exfoliated nanocomposite EVA-NC5B (sample E) decreased by 66% to 15 g/cm^2 s and the mass loss rate curve was spread over 928 s (Fig. 9, curve E), which was less than that observed for the completely exfoliated nanocomposite. The video image (Fig. 10E) also showed black char residue in the pan. Since both samples

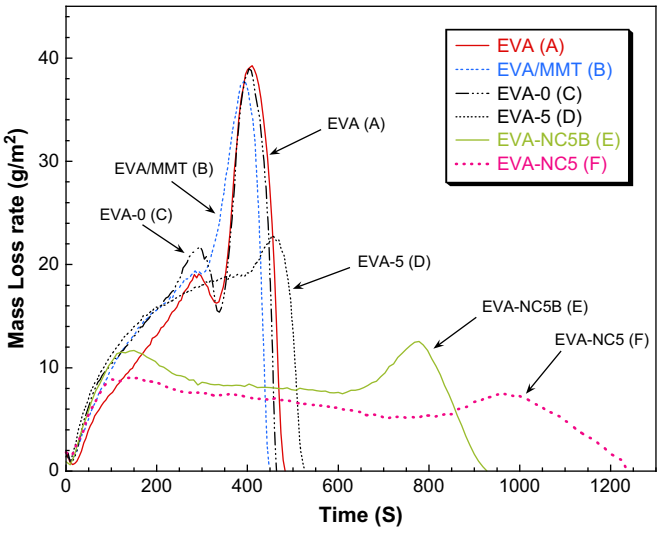

Fig. 9. Mass loss rate plots recorded during gasification at a heat flux of 50 kW/m^2.

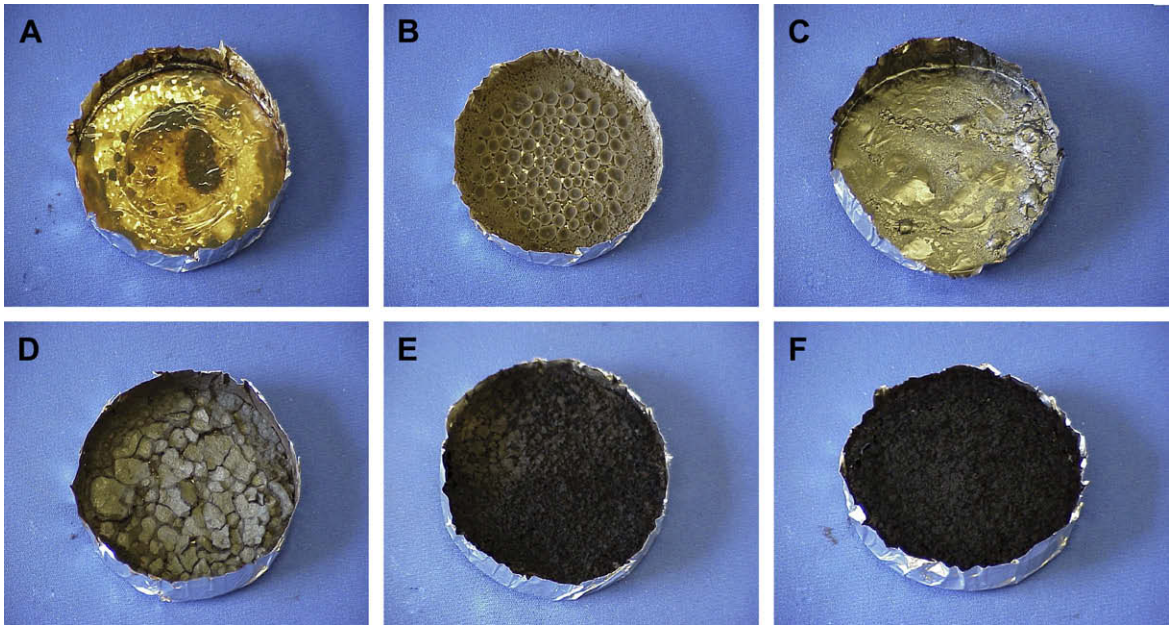

Fig. 10. Video images of the residues after gasification. (A) EVA; (B) EVA/MMT; (C) EVA-0; (D) EVA-5; (E) EVA-NC5B; (F) EVA-NC5.

contained almost the same amount of clay and PVAc, the different gasification behaviors can only be explained by the morphology difference. The homogeneous fully exfoliated nanocomposite clearly exhibited better flame retardancy than the partially exfoliated one, which, in turn, was better than the intercalated nanocomposite.

4. Conclusions

We have reported the mechanical property and flammability study of EVA/MMT nanocomposites prepared via a polymer-modified clay masterbatch approach. We have shown that this approach is unique in accomplishing exfoliated EVA nanocomposites that combined advantages of both polymer blends and polymer composites. The EVA/MMT nanocomposite containing only 5–6% clay exhibited doubled tensile strength and tripled Young's modulus with insignificant decrease in toughness as compared to EVA. We have also shown that the exfoliated EVA nanocomposites exhibited better mechanical properties than the intercalated EVA nanocomposites in almost every aspect. Using a microcalorimetry test (PCFC), we were able to measure the contribution of the components to HRC and THR using milligram-scale samples. Data analysis indicated that both the polymeric modifier and the clay were responsible for the reduction in the flammability of EVA, and that, within experimental error limits, the exfoliated and intercalated materials behaved similarly. Radiant gasification studies of the exfoliated EVA/MMT nanocomposites demonstrated dramatic changes in their mass loss rate curves compared with both EVA and the intercalated EVA/MMT nanocomposite. The homogeneous fully exfoliated nanocomposite showed 80% reduction in peak mass loss rate and more than twice the gasification time. This was not observed in the PCFC test.

Acknowledgement

The authors are grateful to Exxon Mobil for providing the EVA samples. The authors are also grateful to the Cornell Center for Materials Research and Hercules for their facilities and financial support. The technical assistance of Scott Peterson of Texas A&M is gratefully acknowledged.

References

[1] Beyer G. Fire Mater 2001;25(5):193–7.
[2] Gilman JW. Appl Clay Sci 1999;15(1–2):31–49.
[3] Morgan AB, Harris Jr RH, Kashiwagi T, Chyall LJ, Gilman JW. Fire Mater 2002;26(6):247–53.
[4] Gilman JW, Ritchie SJ, Kashiwagi T, Lomakin SM. Fire Mater 1997;21:23–32.
[5] Gilman JW, Lomakin S, Kashiwagi T, VanderHart DL, Nagy V. Fire Mater 1998;22:61–7.
[6] Dabrowski F, Le Bras M, Delobel R, Gilman JW, Kashiwagi T. Macromol Symp 2003;194:201–6.
[7] Beyer G. Fire Mater 2005;29(2):61–6.
[8] Beyer GJ. Fire Sci 2005;23(1):75–87.
[9] Beyer G. Polym Adv Technol 2006;17(4):218–25.
[10] Morgan AB. Polym Adv Technol 2006;17(4):206–17.
[11] Wilkie CA. Recent Adv Flame Retard Polym Mater 2001;12:97–101.
[12] Morgan AB, Wilkie CA. Flame retardant polymer nanocomposites. Hoboken, NJ: John Wiley & Sons; 2007.
[13] Alexandre M, Beyer G, Henrist C, Cloots R, Rulmont A, Jerome R, et al. Macro Rapid Commun 2001;22(8):643–6.
[14] Alexandre M, Beyer G, Henrist C, Cloots R, Rulmont A, Jerome R, et al. Chem Mater 2001;13(11):3830–2.
[15] Zanetti M, Camino G, Mulhaupt R. Polym Degrad Stab 2001;74(3):413–7.
[16] Zanetti M, Camino G, Thomann R, Mulhaupt R. Polymer 2001;42(10):4501–7.
[17] Zanetti M, Kashiwagi T, Falqui L, Camino G. Chem Mater 2002;14(2):881–7.
[18] Morgan AB, Gilman JW, Harris RH, Jackson CL, Wilkie CA, Zhu J. Polym Mater Sci Eng 2000;83:53–4.
[19] La Mantia FP, Lo Verso S, Dintcheva NT. Macromol Mater Eng 2002; 287(12):909–14.
[20] Zhang WA, Chen D, Zhao Q, Ye Fang. Polymer 2003;44(26):7953–61.
[21] Jeon CH, Ryu SH, Chang Y-W. Polym Int 2003;52(1):153–7.
[22] Riva A, Zanetti M, Braglia M, Camino G, Falqui L. Polym Degrad Stab 2002;77(2):299–304.
[23] Li X, Ha C-S. J Appl Polym Sci 2003;87(12):1901–9.
[24] Tang Y, Hu Y, Wang S, Gui Z, Chen Z, Fan W. Polym Degrad Stab 2002;78(3):555–9.
[25] Duquesne S, Jama C, Le Bras M, Delobel R, Recourt P, Gloaguen JM. Compos Sci Technol 2003;63(8):1141–8.
[26] Pramanik M, Srivastava SK, Samantaray BK, Bhowmick AK. Macromol Res 2003;11(4):260–6.
[27] Pramanik M, Srivastava SK, Samantaray BK, Bhowmick AK. J Polym Sci Part B Polym Phys 2002;40(18):2065–72.
[28] Pramanik M, Srivastava SK, Samantaray BK, Bhowmick AK. J Appl Polym Sci 2003;87(14):2216–20.
[29] Zhong Y, Kee DD. Polym Eng Sci 2005;45(4):469–77.
[30] Gelfer MY, Burger C, Chu B, Hsiao BS, Drozdov AD, Si M, et al. Macromolecules 2005;38(9):3765–75.

[31] Peeterbroeck S, Alexandre M, Jerome R, Dubois P. Polym Degrad Stab 2005;90(2):288–94.
[32] Srivastava SK, Pramanik M, Acharya H. J Polym Sci Part B Polym Phys 2005;44(3):471–80.
[33] Prasad R, Gupta RK, Cser F, Bhattcharya SN. J Polym Eng 2005;25(4):305–30.
[34] Prasad R, Gupta RK, Cser F, Bhattacharya SN. J Appl Polym Sci 2006; 101(4):2127–35.
[35] Tang Y, Hu Y, Xiao J, Wang J, Song L, Fan W. Polym Adv Technol 2005; 16(4):338–43.
[36] Lu H, Hu Y, Kong Q, Chen Z, Fan W. Polym Adv Technol 2005;16(9):688–92.
[37] Chaudhary DS, Prasad R, Gupta RK, Bhattacharya SN. Polym Eng Sci 2005; 45(7):889–97.
[38] Chen D, Zhang W, He P. Polym Polym Compos 2005;13(3):271–80.
[39] Fang P, Chen Z, Zhang S, Wang S, Wang L, Feng J. Polym Int 2006;55(3):312–8.
[40] Ardhyananta H, Ismail H, Takeichi T, Judawisastra H. Polym Plast Technol Eng 2006;45(12):1285–93.
[41] Ran Q, Hua H, Tian Y, Wu S, Shen J. Polym Polym Compos 2006;14(3):301–6.
[42] Szep A, Szabo A, Tosh N, Anna P, Marosi G. Polym Degrad Stab 2006;91(3):593–9.
[43] Xie W, Gao Z, Pan W-P, Hunter D, Singh A, Vaia R. Chem Mater 2001;13:2979–90.
[44] Xie W, Xie R, Pan W-P, Hunter D, Koene B, Tan L-S, et al. Chem Mater 2002; 14:4837–45.
[45] Davis RD, Gilman JW, VanderHart DL. Polym Degrad Stab 2003;79(1):111–21.
[46] Xi Y, Zhou Q, Frost RL, He H. J Colloid Interface Sci 2007;311(2):347–53.
[47] Beyer G. Fire Mater 2002;26(6):291–3.
[48] Shi Y, Peterson S, SD Y. Chem Mater 2007;19(7):1552–64.
[49] Shi Y. Diss Abstr Int, B 2006;66(9):4839.
[50] Austin PJ, BR R, Kashiwagi T. Fire Mater 1998;22:221–37.
[51] Kashiwagi T, Harris J, Richard H, Zhang X, Briber RM, Cipriano BH, et al. Polymer 2004;45:881–91.
[52] Lyon RE, Walters RN. US Patent 5,981,290; 1999. p. 9.
[53] Lyon RE. US Patent 6,464,391; 2002. p. 9.
[54] Lyon RE, Walters RN, Gandhi S. Recent Adv Flame Retard Polym Mater 1998; 9:334–53.
[55] Lyon RE, Walters RN. J Anal Appl Pyrolysis 2004;7:27–46.
[56] Walters RN, Lyon RE. J Appl Polym Sci 2003;87(3):548–63.
[57] Lin TS, Cogen JM, Lyon RE. Proceedings of international wire and cable symposium, Orlando, FL; 2007. p. 176–85.
[58] Schartel B, Pawlowski KH, Lyon RE. Thermochim Acta 2007;462:1–14.